Case Series

Imaging of extranodal lymphomas in the head and neck: A case series and review of the literature

Chad Pierre Issa[1], Amberly Nunez[2], Rula Mualla[3], Sagar Kansara[3]

[1]School of Medicine, Louisiana State University Health Sciences Center, New Orleans, [2]Department of Pathology, Pathology Group of Louisiana, [3]Department of Otolaryngology – Head and Neck Surgery, Louisiana State University Health Sciences Center, Our Lady of the Lake Regional Medical Center, Baton Rouge, United States.

*Corresponding author:
Sagar Kansara,
Department of Otolaryngology – Head and Neck Surgery, Louisiana State University Health Sciences Center, Our Lady of the Lake Regional Medical Center, Baton Rouge, United States.

skans1@lsuhsc.edu

ABSTRACT

Extranodal lymphomas (ENLs) are relatively rare malignancies of the head and neck. Clinical presentation varies greatly depending on location, pattern of nodal involvement, and histologic subtype. The most frequently involved sites include the palatine tonsils and nasal cavity/paranasal sinuses, and over half of patients have concurrent nodal disease. Most are non-Hodgkin's lymphomas of B-cell lineage. While the clinical presentation may mimic other pathologies of the head and neck, various radiographic features and patterns may help raise suspicion for ENL as a differential consideration. This is of critical importance given that the management and treatment of lymphomas differ significantly from other pathologies of the head and neck. In this case series, three cases of ENL in the head and neck are described, with an emphasis on radiographic findings. A review of epidemiology and treatment paradigms is also provided.

Keywords: Lymphoma, Cancer, B-cell, Case series, Literature review

INTRODUCTION

Hodgkin's and non-Hodgkin's lymphomas (NHLs) are relatively uncommon and represent <5% of all head and neck malignancies.[1] They may arise from any location in the head and neck and display either a nodal, extranodal, or combined nodal-extranodal pattern on imaging. Following the gastrointestinal tract, the head–and-neck region is the second most common site of extranodal lymphomas (ENLs) in the body.[2] The most frequently involved sites include the palatine tonsils, nasal cavity/paranasal sinuses, and the nasopharynx.[3] The majority are of B-cell lineage, with diffuse B-cell lymphoma (BCL) being the most common histologic subtype.[1] As opposed to Hodgkin's lymphoma, which most frequently presents as painless cervical lymphadenopathy without extranodal involvement, the presentation of NHL in the head and neck is much more variable with extranodal involvement seen in up to 30% of cases.[1] Since NHL frequently appears in extranodal sites, the clinical presentation and radiographic findings can be difficult to differentiate from other pathologies of the head and neck. Here, we describe three cases of extranodal NHL in the head and neck, with an emphasis on radiologic findings, and provide a review of the literature.

CASE SERIES

Case 1

A 55-year-old female with a medical history of transient ischemic attack and tobacco abuse (60-pack-year smoking history, current smoker) presented with a 1-month history of

progressively worsening left-sided throat pain and dysphagia to solids. She had previously received a 7-day course of oral amoxicillin followed by a 6-day course of oral azithromycin and a steroid injection without any improvement in symptoms. Physical examination was significant for the left level I–III cervical lymphadenopathy, and flexible endoscopy, further, revealed a left lingual tonsillar mass with ipsilateral base of the tongue involvement [Figure 1a].

Computed tomography (CT) scan showed a 5.9 × 4.8 × 8 cm left-sided oropharyngeal (OP) mass with extension to the floor of the mouth anteriorly, lateral to the internal carotid laterally, and below the level of the hyoid bone inferiorly. There were also multiple enlarged left cervical lymph nodes in the submandibular and level II–III regions [Figure 1b and c]. The parotid, submandibular, and thyroid glands appeared normal. No abnormalities were seen in the chest.

Given the high suspicion of OP malignancy, the patient opted for an in-office biopsy of the left tonsillar lesion at her initial visit. Final pathology ultimately returned showing high-grade BCL (proliferative rate of 80% by Ki-67; cluster of differentiation 20 [CD-20], and BCL-2 positive; BCL-6, CD-5, and CD-10 negative) [Figure 2]. The patient was subsequently referred to medical oncology and completed six cycles of rituximab, cyclophosphamide, doxorubicin, vincristine, and prednisone (R-CHOP) immunochemotherapy.

Case 2

A 64-year-old male with a history of hypertension, hyperlipidemia, and tobacco abuse (30 pack-year smoking history, quit 3 years ago) presented for further evaluation of a right tonsillar mass previously identified by an otolaryngologist at an outside facility. Patient history was significant for a 2-month history of progressively worsening

sore throat, dysphagia to both solids and liquids, and right-sided otalgia. On physical examination, the patient was noted to have significant right level II–III cervical lymphadenopathy (at least three palpable nodes, largest ~ 3 cm), and in-office endoscopy revealed a large lesion of the right palatine tonsil with involvement of the glossotonsillar sulcus inferiorly and the posterior surface of the soft palate superiorly.

Fluorodeoxyglucose positron-emission tomography CT (FDG PET-CT) imaging showed a hypermetabolic neoplasm at the right palatine tonsil measuring 3.7 × 2.4 cm with standardized uptake value (SUV) of 32.5 extending to the soft palate superiorly associated with the right level II and level III lymphadenopathy measuring up to 3.2 × 1.5 cm with SUV of 22.7 and 2.4 × 2.0 cm with SUV of 26.9, respectively [Figure 3]. There was also a single left level II node medial to the parotid tail measuring 1.4 × 0.5 cm with SUV of 2.6 which was questionable for tumor involvement [Figure 3d]. There was no evidence of distant metastasis.

Direct laryngoscopy with biopsy of the tonsillar mass was performed in the operating room and biopsy results returned showing high-grade BCL (proliferative rate of 90% by Ki-67; CD-20, BCL-2, BCL-6, and MUM-1 positive; CD-5 and CD-10 negative) [Figure 4]. The patient was subsequently referred to medical and radiation oncology and received three cycles of R-CHOP immunochemotherapy followed by consolidative radiation therapy.

Case 3

A 79-year-old male with medical history of pulmonary embolism and tobacco abuse (50-pack-year smoking history, former smoker) was referred for further evaluation of an enlarging left neck mass that had been present for at least 4 months. Patient history was also significant for persistent
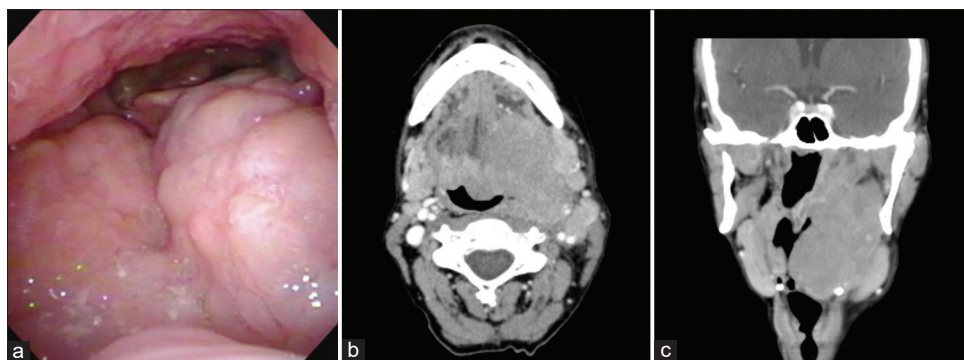

Figure 1: A 55-year-old female with the left tonsillar lymphoma. (a) In-office nasopharyngoscopy shows enlargement of the left lingual tonsil. (b) Axial CT image of the neck with contrast shows a large, homogenous, minimally-enhancing left oropharyngeal mass extending into the floor of the mouth anteriorly and lateral to the internal carotid artery laterally. (c) Coronal CT image shows the same oropharyngeal mass extending below the level of the hyoid inferiorly. There were also multiple enlarged left cervical lymph nodes in the submandibular and level II–III regions. CT: Computed tomography.
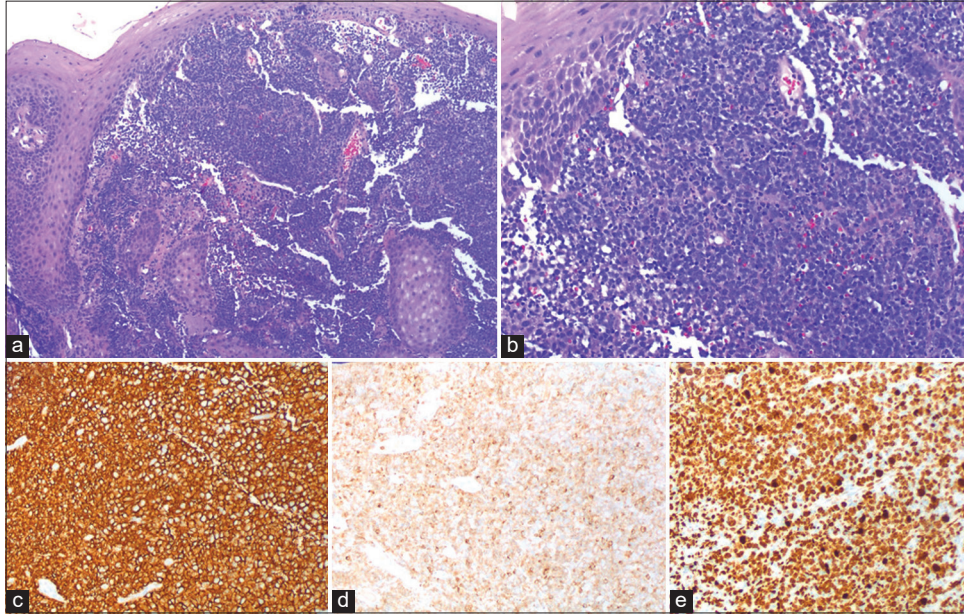
Figure 2: A 55-year-old female with the left tonsillar lymphoma. (a) Low power H&E-stained section of the tonsil biopsy shows overlying squamous epithelium and underlying proliferation of abnormal lymphocytes with effacement of the normal tonsil architecture (10x). (b) Intermediate power H&E-stained section shows an infiltrate consisting of intermediate to large lymphoid cells with scant cytoplasm and occasional prominent nucleoli (40x). (c) CD-20 and (d) BCL-2 IHC staining demonstrate diffuse membranous positivity and weak cytoplasmic staining, respectively (40x). (e) Ki-67 IHC staining shows strong nuclear staining in approximately 80% of the lymphoma cells (40x). H&E: Hematoxylin and eosin, IHC: Immunohistochemical, CD-20: Cluster of differentiation 20 (a common B-cell marker), BCL-2: B-cell lymphoma 2 (an anti-apoptotic protein in which overexpression increases the lifespan of B-cells), Ki-76: Antigen Kiel 67 (a cellular proliferation marker).

left-sided nasal obstruction and B-symptoms including chills, drenching night sweats, and unintentional weight loss of 40–50 pounds over the past year. On physical exam, the patient was noted to have extensive left level II-IV cervical lymphadenopathy, and in-office endoscopy revealed a flesh-colored mass appearing from the left sphenoethmoidal recess.

CT imaging showed a 2 cm mass within the left posterior ethmoid and sphenoid sinuses with extension into the pterygopalatine fossa [Figure 5a-d], extensive left level II–IV necrotic cervical lymphadenopathy with conglomerate nodes measuring up to 3.1 × 3.5 × 7.8 cm [Figure 5e], and prominent right paratracheal lymph nodes. A 1.2 × 2.0 cm spiculated nodular density with associated microcalcifications was also noted in the apex of the left lung. Magnetic resonance imaging (MRI) performed weeks later showed thickening with enhancement of the left posterior ethmoid and sphenoid sinuses [Figure 5f-h], prominence of the left posterior aspect of the middle turbinate, and two small enhancing masses in the cerebral white matter with surrounding edema (3 mm mass in the right frontal lobe and a 5 mm mass in the left parietal lobe) [Figure 5i and j]. There was no evidence of direct intracranial extension or orbital

abnormalities. Subsequent FDG PET-CT performed for staging also showed a left posterior ethmoid and sphenoid sinus soft-tissue density (SUV max of 14.3) and extensive left cervical lymphadenopathy (SUV max of 25.1) as well as extensive FDG-avid disease throughout the thorax including coalescing large nodular masses filling the entirety of the left lower lobe and lingula (measuring 14.0 × 7.6 × 9.0 cm with SUV max of 28.3), multiple left pleural nodules, large right lower lobe pulmonary nodules (the largest measuring 2.3 × 1.9 cm with SUV max of 21.9), and mediastinal and left hilar lymphadenopathy (the largest lymph node being a right peritracheal lymph node measuring 2.3 × 2.6 cm with SUV max 24.9). There were also multiple FDG-avid skin nodules in the thorax and abdomen (the largest being a left flank skin nodule measuring 16 × 12 mm with SUV max of 11.0).

Nasal endoscopy with biopsy and direct laryngoscopy was performed in the operating room. Frozen sections of the sphenoethmoidal mass returned as sinonasal undifferentiated carcinoma versus lymphoma, and final pathology showed high-grade B-lineage lymphoma (proliferative rate of 85% by Ki-67; CD-20, BCL-2, and BCL-6 positive; and CD-5 and CD-10 negative) [Figure 6]. A subsequent ultrasound-guided biopsy of the left cervical mass was performed for appropriate
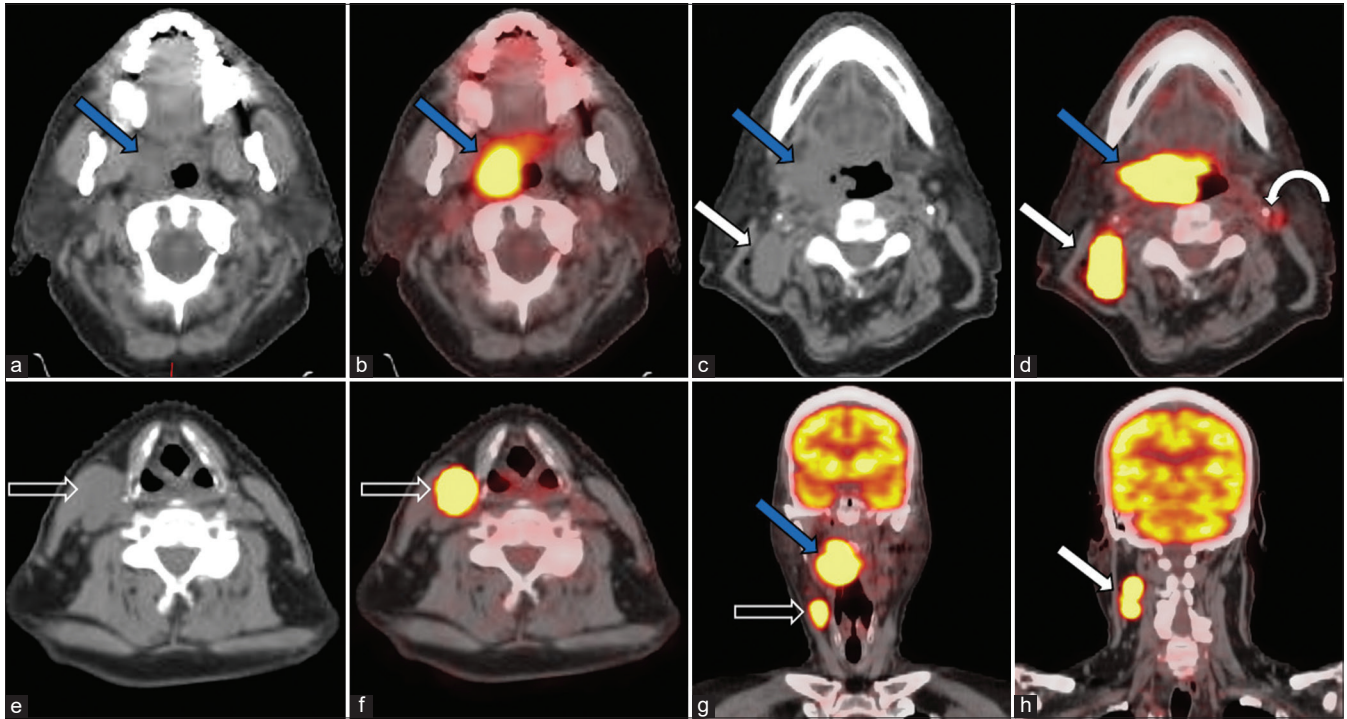
Figure 3: A 64-year-old male with right tonsillar lymphoma. (a) Axial CT and (b) FDG PET-CT imaging shows a hypermetabolic mass at the right palatine tonsil (straight blue arrows) measuring 3.7 x 2.4 cm with SUV of 32.5 extending to the soft palate superiorly. (c) Axial CT and (d) FDG PET-CT images at the level of the mandible also show the mass at the right palatine tonsil (straight blue arrows) and right level II lymphadenopathy (straight white arrows) measuring up to 3.2 x 1.5 cm with SUV of 22.7. There is also a single left level II lymph node medial to the parotid tail (curved white arrow) measuring 1.4 x 0.5 cm with SUV of 2.6 which is questionable for tumor involvement. (e) Axial CT and (f) FDG PET-CT images at the level of the thyroid cartilage shows right level III lymphadenopathy (straight empty arrows) measuring 2.4 x 2.0 cm with SUV of 26.9. Coronal FDG PET-CT (g and h) images also showing the palatine tonsillar mass (straight blue arrow), cervical level III lymphadenopathy (straight empty arrow), and cervical level II lymphadenopathy (straight white arrow). CT: computed tomography; FDG PET-CT: 18-fluorodeoxyglucose positron-emission tomography computed tomography; SUV: standardized uptake value.
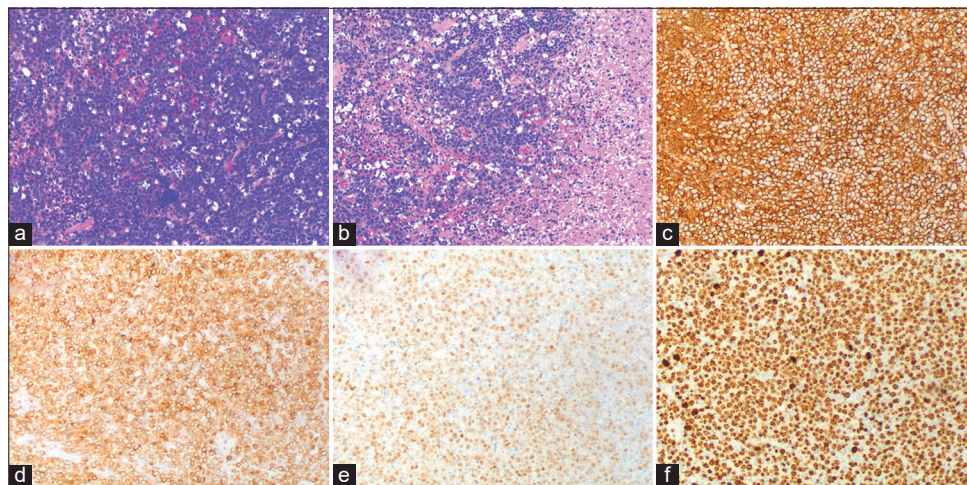

Figure 4: A 64-year-old male with the right tonsillar lymphoma. (a) Intermediate power view of an H&E-stained section of the tonsil biopsy shows atypical large lymphocytes with small mature lymphocytes scattered amongst the atypical lymphocytes (40x). (b) Intermediate power view of another section shows an infiltrate of intermediate to large lymphoid cells, admixed histiocytes, and prominent necrosis (right side of image) (40x). IHC staining shows cells that are positive for (c) cluster of differentiation 20, (d) B-cell lymphoma-2, (e) and MUM-1 (40x). (f) Ki-67 IHC staining shows strong nuclear staining in approximately 90% of the lymphoma cells (40x). H&E: Hematoxylin and eosin, IHC: Immunohistochemical, MUM-1: Multiple myeloma-1.
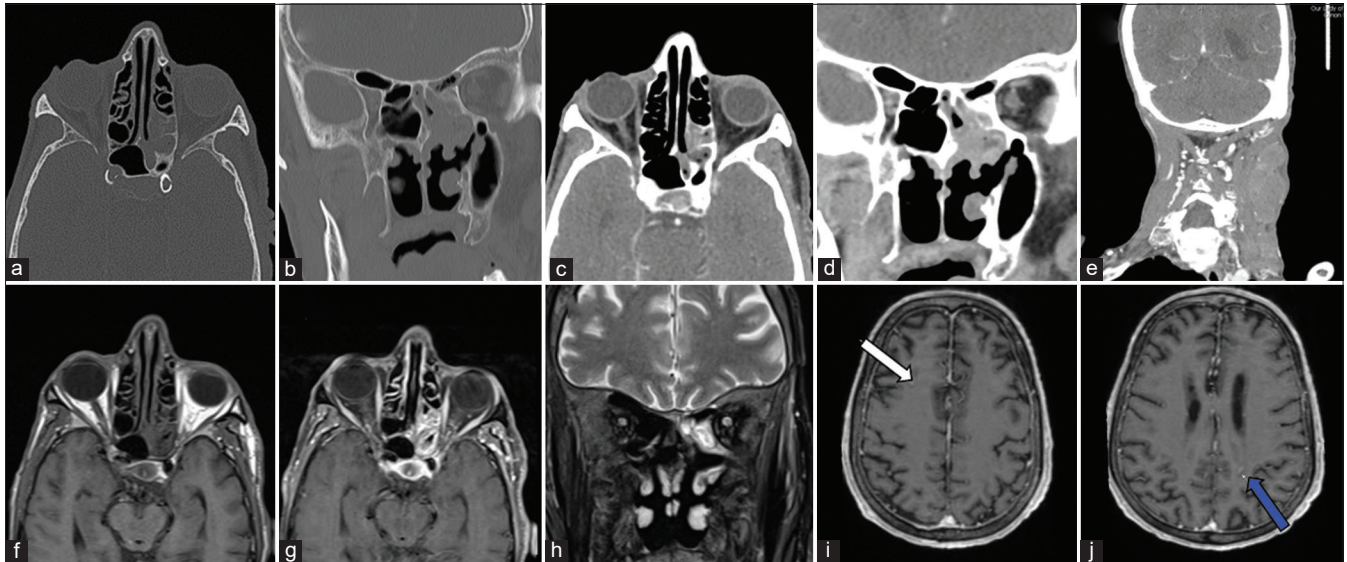
Figure 5: A 79-year-old male with the left posterior ethmoid and sphenoid sinus lymphoma. (a) Axial and (b) coronal CT scan of the sinuses/facial bones without contrast shows a homogenous soft-tissue mass involving the left posterior ethmoid and sphenoid sinuses. Following contrast administration (c and d), the mass demonstrates mild, relatively uniform enhancement. There is no evidence of intracranial or intraorbital extension. (e) CT of the neck with contrast shows extensive left level II–IV necrotic cervical lymphadenopathy with conglomerate nodes. (f) Axial T1-weighted MRI shows a homogenous, hypointense mass involving the left posterior ethmoid and sphenoid sinuses. Post-gadolinium (g) axial T1-weighted and (h) coronal T2-weighted MRI show intense enhancement of the mass. The overall mass-like appearance on MRI shows improvement relative to the previous CT, which may indicate that there was trapped surrounding fluid which has since improved. (i) Axial reformat MRI shows a small enhancing mass in the right frontal lobe (straight white arrow), and (j) another axial reformat MRI shows a small enhancing mass in the left parietal lobe (straight blue arrow). CT: Computed tomography, MRI: magnetic resonance imaging.
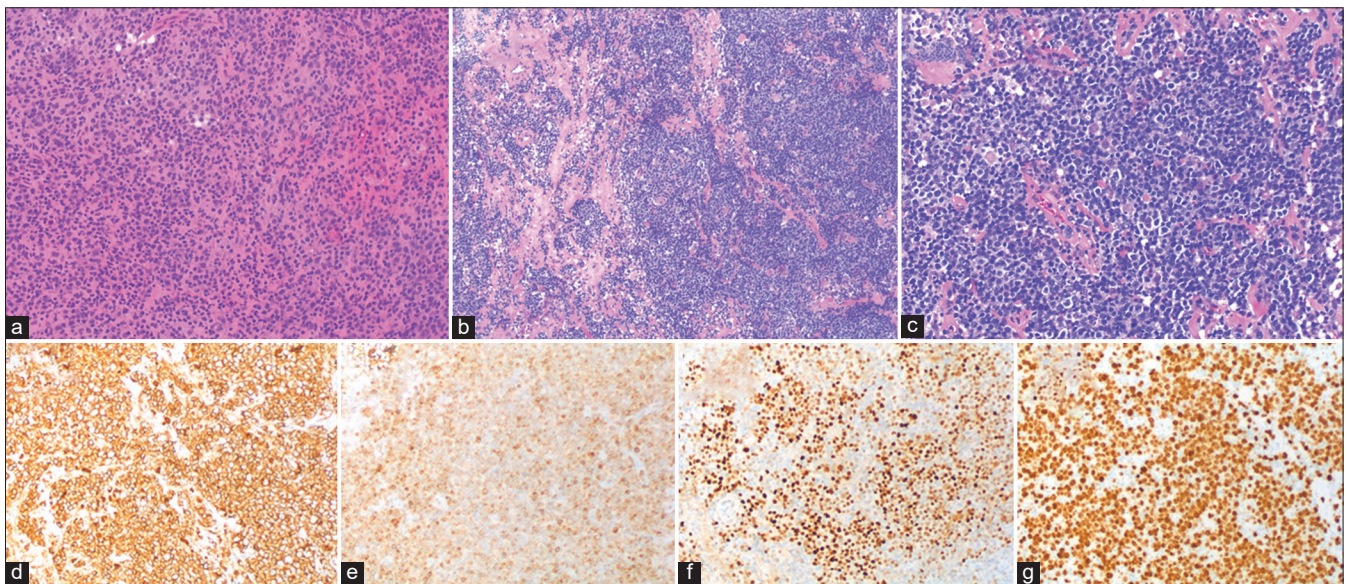

Figure 6: A 79-year-old male with the left posterior ethmoid and sphenoid sinus lymphoma. (a) Intermediate power view of an H&E-stained frozen section of the sphenoid/ethmoid mass biopsy shows sheets of variably sized lymphocytes (40x). (b) Low power view of an H&E-stained section shows predominantly large lymphocytes with intermixed fibrosis (10x), and an (c) intermediate power view shows an infiltrate of large lymphocytes with irregular nuclear membranes, prominent nucleoli, and scant cytoplasm (40x). IHC staining shows tumor cells that are positive for (d) Cluster of differentiation 20, (e) BCL-2, and (f) BCL-6. (g) Ki-67 IHC staining shows strong nuclear staining in approximately 85% of the lymphoma cells (40x). H&E: Hematoxylin and eosin, IHC: Immunohistochemical, BCL: B-cell lymphoma.

treatment planning, which ultimately confirmed NHL nodal involvement. The patient was referred to medical oncology for further evaluation and treatment planning. He completed two cycles of R-CHOP immunochemotherapy; however, he experienced a prolonged hospitalization due to septic pneumonia which delayed treatment. R-CHOP with dose modification or second-line treatment is being considered, given his intolerance to first-line management.

DISCUSSION

ENLs of the head and neck are rare with an annual incidence rate of <6/100,000.[4] The great majority are NHLs.[1] Clinical presentation varies greatly depending on location, pattern of nodal involvement, and histologic subtype. The most frequent sites of extranodal involvement include the oropharynx (particularly the palatine and lingual tonsils of Waldeyer's ring) and the nasal cavity/paranasal sinuses, and approximately half of patients present with associated nodal disease.[3] Overall, ENLs tend to be of B-cell lineage, with DLBCL being the most common histologic subtype.[1] In Cases 1–2 and Case 3, the sites of extranodal involvement were the oropharynx and the nasal cavity/paranasal sinuses, respectively. All three cases described also had concomitant nodal disease and were ultimately diagnosed with high-grade BCLs.

Imaging plays a critical role in the initial diagnosis, staging, treatment planning, response assessment, and surveillance of head and neck tumors, including ENLs. Contrast-enhanced CT (CECT) is the first-line imaging modality for the initial evaluation of tumor extent and the detection of adjacent osseous involvement. It is also the preferred modality for staging and assessing treatment response in FDG non-avid lymphomas. MRI with and without contrast is also frequently performed, particularly for tumors of the nasal cavity and paranasal sinuses, as it provides superior soft-tissue detail and allows for detailed assessment of intracranial, intra-orbital, and transfascial extension (e.g., pterygopalatine and infratemporal fossae). At most institutions, FDG PET is routinely performed for the pre-treatment staging of most lymphomas and is also used for the detection of disease recurrence. More recently, FDG PET-CT has become an important imaging modality in the workup and management of head and neck tumors, especially for FDG-avid tumors and lymphomas.

While excisional biopsy with histopathological examination remains the standard for establishing a definitive diagnosis, various features and patterns can be suggestive of ENL. This may be of critical importance given that the management and treatment of lymphoma differ significantly from other pathologies of the head and neck. On CT imaging, ENLs classically appear as a homogenous mass of similar density to surrounding soft tissues and demonstrate variable, uniform enhancement following contrast administration.[1,5] On MRI, they tend have low-signal intensity on T1-weighted (T1w) sequences and variable signal intensity on T2-weighted (T2w) sequences relative to muscle.[1,5] In general, ENLs are non-necrotic and rarely destroy surrounding anatomical structures.[1] From an imaging perspective, the determination of the anatomical site from which the tumor originated is essential for establishing a list of differential diagnoses (and to consider each of their respective radiographic appearances). More so, ENLs are commonly described in the literature based on the head and neck subsite involved.

OP lymphomas most frequently occur in the lymphoid tissues of the palatine (>70%) and lingual (>20%) tonsils.[3] Involvement of multiple anatomical subsites is relatively common (e.g., simultaneous involvement of the palatine and lingual tonsils) and may occur unilaterally or bilaterally.[6] Most OP lymphomas tend to be submucosal, and therefore, initial tumor growth in this region is often undetectable.[6] In a 2010 case series of 12 patients, Wang *et al.* reported that the majority (58%) of patients presented late (defined as a mass >4 cm), with dysphagia and sore throat being the most common presenting symptoms.[7] OP lymphomas typically present with classic radiographic features of ENL. On CECT and conventional T1/T2w MRI, they most commonly appear as a large, well-demarcated, homogenous mass with similar intensity to normal tonsillar tissue and display minimal, uniform enhancement following contrast administration.[1] The tumors rarely demonstrate ulceration or central necrosis, and they tend to spread along the pharyngeal wall and displace, rather than invade, local anatomical structures.[1] In a 2014 case series of eight patients with palatine tonsillar lymphoma, King *et al.* reported that only 12.5% (*n* = 1) presented with direct invasion of nearby structures, with displacement being significantly more common (87.5%).[8] OP ENLs have the highest incidence of associated cervical lymph node (bilateral > unilateral) involvement compared to ENLs in other locations and is seen in over half of patients.[9] Nodal necrosis is uncommon and occurs in <10% of patients.[6] The two patients with tonsillar lymphoma (Cases 1–2) displayed all the classic radiologic features of OP lymphomas.

The top differential diagnosis is OP squamous cell carcinoma (SCC). Like OP lymphomas, OP SCCs have a predilection for the palatine tonsillar region and the base of the tongue, and due to their ability to grow silently initially, most patients also present at more advanced stages with cervical lymph node metastasis.[10] Various imaging features are more suggestive of SCC rather than lymphoma. In general, OP SCCs tend to appear more heterogenous and frequently demonstrate ulceration, central necrosis, and invasion of local soft tissues and bone.[1,6] Likewise, they are also more commonly associated with cervical lymph node necrosis.[11] It is worth

noting, however, that enlarged cervical lymph nodes in NHL frequently demonstrate necrosis following the initiation of treatment, which is an indication of a favorable response to therapy.[8] Another important differential consideration in this region is lymphoid hypertrophy, which more frequently involves the nasopharynx rather than the oropharynx and is indistinguishable from lymphoma using imaging alone.[12]

Sinonasal lymphomas are broadly classified into two major subtypes, including BCLs and T/NK-cell lymphomas. BCLs are the most common subtype overall and tend to carry a more favorable prognosis, whereas T/NK-cell lymphomas are more common in Asia and South America and have a strong association with prior Ebstein-Barr Virus infection.[1] In general, sinonasal lymphomas tend to arise within the nasal cavity, and less frequently, the maxillary sinus.[1] Involvement of the ethmoid and sphenoid sinuses, as seen in Case 3, is extremely rare.[1] On CECT and MRI with and without contrast, low-grade lymphomas classically present as a relatively large (>2 cm), homogenous, non-invasive soft-tissue mass with minimal, uniform enhancement.[1,13] However, the appearance of high-grade forms is often non-specific and may mimic other aggressive malignancies and inflammatory disorders.[13] High-grade BCLs commonly present with invasion into extrasinus spaces (e.g., pterygopalatine fossa) and destruction of the bony orbit, and T/NK-cell lymphomas frequently present with destruction to the midline structures, particularly the nasal septum and nasal turbinates.[1,13,14] Ill-defined tumor margins, central necrosis, and non-uniform enhancement may also be seen on imaging.[15]

Given that sinonasal lymphomas are extremely rare and account for <1% of all ENL cases,[13] the presence of a sinonasal mass should generally raise suspicion for SCC. Apart from typically originating from the paranasal sinuses rather than the nasal cavity,[1] multiple studies have revealed various other differences between sinonasal SCC and NHL on imaging. In a 2022 comparative study, Maitra and Singh reported that the presence of intratumoral necrosis (87.5% vs. 18.18%, *P* < 0.0001) and destructive growth (83.33% vs. 27.27%, *P* = 0.0009) on CT were significantly more common in sinonasal SCC than NHL.[16] In another study, Kim *et al.* reported that NHL had larger tumor volumes, greater tumor homogeneity on T2-weighted MR sequences, and a lower apparent diffusion coefficient compared to sinonasal SCC.[17] While cervical lymph node involvement is uncommon in both sinonasal NHL and SCC, with rates ranging between 9% and 30%, the presence of nodal necrosis is highly suspicious for SCC.[17,18] Accordingly, the presence of significant nodal necrosis in Case 3 raised suspicion for a second primary head and neck malignancy; however, subsequent nodal biopsy ultimately confirmed NHL nodal involvement. Two other important differential considerations in the sinonasal region include Wegener's granulomatosis, which typically also

involves the lungs and kidneys, and olfactory neuroblastoma, which typically appears as a heterogeneous mass at the olfactory groove with multiple peritumoral cysts.[12] Another less common differential consideration is a granulocytic sarcoma (commonly referred to as chloroma), which is a malignant soft-tissue tumor composed of myeloid cells and typically occurs in patients with acute myeloid leukemia.[19] These tumors have a predilection for the orbit and paranasal sinuses when occurring in the head and neck region and frequently include tumor deposits in the lungs, pleura, mediastinum, and skin, all of which were also seen in Case 3.[19,20] Imaging findings for chloromas on CT, MRI, and FDG PET-CT are non-specific and indistinguishable from other malignancies, including lymphomas, and biopsy is required for definitive diagnosis.[19,20]

Although there is no pathognomonic finding for ENL at a particular anatomical subsite, or in the head-and-neck region in general, knowledge of their radiographic appearances may increase one's suspicion for lymphoma in clinical practice and help distinguish it from other head and neck pathologies until more sophisticated imaging techniques are developed. Recently, Maeda *et al.* reported the utilization of diffusion-weighted MRI to differentiate NHL from SCC with accuracy rates >90%.[21] Similarly, other studies have developed radiomic nomograms to differentiate the two, incorporating both imaging and patient characteristics into their algorithms, with promising results.[22] Other innovative imaging modalities and techniques warrant further investigation to elucidate their role in characterizing head and neck lymphomas.

Beyond the importance of imaging in the initial evaluation and diagnosis of head and neck NHLs, it plays a crucial role in the staging and assessment of treatment response. FDG PET-CT is now considered the gold standard for FDG-avid lymphomas and CECT is preferred for variably FDG-avid lymphomas.[23] The Ann Arbor Staging System, which stages lymphomas based on the extent of nodal involvement (consists of four stages, I–IV), is used to guide management along with consideration of prognostic and risk factors.[23] In general, patients with limited disease (typically defined as Ann Arbor stage I or II with tumor size <7.5 cm) undergo an abbreviated treatment course with three cycles of R-CHOP immunochemotherapy therapy followed by involved-field radiation therapy.[24] In patients who present with advanced disease (approximately 70% of cases), six cycles of R-CHOP immunochemotherapy with or without radiation are considered the standard treatment.[24] The details of management in the setting of refractory and/or relapsed cases, indications for second-line regimens including platinum-based therapies and targeted-based approaches, and other patient-specific scenarios are beyond the scope of this review and are described elsewhere.[24]

The Lugano Classification criteria of 2014, developed primarily based on expert opinion to help standardize the interpretation of imaging results, is currently the most widely used response assessment criteria by clinicians, clinical trials, and regulatory agencies for lymphomas.[23,25] The system incorporates the Deauville 5-Point Scale and consists of four classifications based on tumor avidity relative to the mediastinum and liver on FDG PET-CT and bidimensional tumor measurements on CT imaging.[23] This system differs from other popular response criteria including Response Evaluation Criteria in Solid Tumors, a widely adopted standardized method of assessing response in solid tumors using unidimensional (rather than bidimensional) tumor measurements on CT imaging, and PET Evaluation Response Criteria in Solid Tumors, a method of assessing response using quantitative, objective measurements of tumor FDG avidity (rather than subjective comparison to the mediastinum and liver) on FDG PET-CT imaging.[23,25,26] Most recently, the International Working Group proposed Response Evaluation Criteria in Lymphoma in 2017, which includes unidimensional tumor measurements to align the response criteria for lymphomas with that of solid tumors and to decrease subjectivity involved in bidimensional measurements.[25] Altogether, these tools allow for a more standardized and objective evaluation of response to treatment.

It is important to note that there are limitations to this case series as well as the role of imaging in the workup and management of ENLs. Although this series describes three cases at a single institution and consequently limits the generalizability of this study, the literature review provided expands on the classically associated imaging findings of head and neck ENLs. Despite this, ENLs still may present with uncharacteristic imaging findings as demonstrated in Case 3. In addition, as stated previously, definitive diagnosis cannot be obtained exclusively through imaging, emphasizing the importance of the interplay between imaging and histopathology.

CONCLUSION

Three cases of ENL in the head and neck are described. While the clinical and radiographic presentations of ENLs can be highly variable, various imaging features and patterns may help raise suspicion for ENL. Knowledge of these features is crucial given that diagnosis and further management of lymphomas differs significantly from other head-and-neck pathologies. Imaging plays a fundamental role in understanding disease staging, monitoring treatment response, and in surveillance of ENL.

Ethical approval

Institutional Review Board approval is not required.

Declaration of patient consent

The authors certify that they have obtained all appropriate patient consent.

Financial support and sponsorship

Nil.

Conflicts of interest

There are no conflicts of interest.

Use of artificial intelligence (AI)-assisted technology for manuscript preparation

The authors confirm that there was no use of artificial intelligence (AI)-assisted technology for assisting in the writing or editing of the manuscript and no images were manipulated using AI.

REFERENCES

1. Kwok HM, Ng FH, Chau CM, Lam SY, Ma JK. Multimodality imaging of extra-nodal lymphoma in the head and neck. Clin Radiol 2022;77:e549-59.
2. Vega F, Lin P, Medeiros LJ. Extranodal lymphomas of the head and neck. Ann Diagn Pathol 2005;9:340-50.
3. Kuo CY, Shih CP, Cheng LH, Liu SC, Chiu FH, Lin YY, *et al.* Head and neck lymphomas: Review of 151 cases. J Med Sci 2020;40:215-23.
4. Picard A, Cardinne C, Denoux Y, Wagner I, Chabolle F, Bach CA. Extranodal lymphoma of the head and neck: A 67-case series. Eur Ann Otorhinolaryngol Head Neck Dis 2015;132:71-5.
5. Mahmoud EM, Howard E, Ahsan H, Cousins JP, Nada A. Cross-sectional imaging evaluation of atypical and uncommon extra-nodal head and neck Non-Hodgkin lymphoma: Case series. J Clin Imaging Sci 2023;13:6.
6. Zhang CX, Liang L, Zhang B, Chen WB, Liu HJ, Liu CL, *et al.* Imaging anatomy of Waldeyer's Ring and PET/CT and MRI findings of oropharyngeal non-Hodgkin's lymphoma. Asian Pac J Cancer Prev 2015;16:3333-8.
7. Wang XY, Wu N, Zhu Z, Zhao YF. Computed tomography features of enlarged tonsils as a first symptom of non-Hodgkin's lymphoma. Chin J Cancer 2010;29:556-60.
8. King AD, Lei KI, Ahuja AT. MRI of primary non-Hodgkin's lymphoma of the palatine tonsil. Br J Radiol 2001;74:226-9.
9. Rayess HM, Nissan M, Gupta A, Carron MA, Raza SN, Fribley AM. Oropharyngeal lymphoma: A US population based analysis. Oral Oncol 2017;73:147-51.
10. Chi AC, Day TA, Neville BW. Oral cavity and oropharyngeal squamous cell carcinoma-an update. CA Cancer J Clin 2015;65:401-21.
11. Seeburg DP, Baer AH, Aygun N. Imaging of patients with head and neck cancer: From staging to surveillance. Oral Maxillofac Surg Clin North Am 2018;30:421-33.

12. Watal P, Bathla G, Thaker S, Sato TS, Moritani T, Smoker WR. Multimodality imaging spectrum of the extranodal lymphomas in the head and neck-a pictorial review. Curr Probl Diagn Radiol 2018;47:340-52.

13. Aiken AH, Glastonbury C. Imaging Hodgkin and non-Hodgkin lymphoma in the head and neck. Radiol Clin North Am 2008;46:363-78.

14. Ooi GC, Chim CS, Liang R, Tsang KW, Kwong YL. Nasal T-cell/natural killer cell lymphoma: CT and MR imaging features of a new clinicopathologic entity. Am J Roentgenol 2000;174:1141-5.

15. Chen Y, Wang X, Li L, Li W, Xian J. Differential diagnosis of sinonasal extranodal NK/T cell lymphoma and diffuse large B cell lymphoma on MRI. Neuroradiology 2020;62:1149-55.

16. Maitra M, Singh MK. A comparative study on clinico-radiological differentiation of sino-nasal squamous cell carcinoma (SCC) and sino-nasal non-Hodgkins lymphoma (NHL). Indian J Otolaryngol Head Neck Surg 2022;74:142-5.

17. Kim SH, Mun SJ, Kim HJ, Kim SL, Kim SD, Cho KS. Differential diagnosis of sinonasal lymphoma and squamous cell carcinoma on CT, MRI, and PET/CT. Otolaryngol Neck Surg 2018;159:494-500.

18. Koeller KK. Radiologic features of sinonasal tumors. Head Neck Pathol 2016;10:1-12.

19. Magdy M, Abdel Karim N, Eldessouki I, Gaber O, Rahouma M, Ghareeb M. Myeloid sarcoma. Oncol Res Treat 2019;42:219-24.

20. Singh A, Kumar P, Chandrashekhara SH, Kumar A. Unravelling chloroma: Review of imaging findings. Br J Radiol 2017;90:20160710.

21. Maeda M, Kato H, Sakuma H, Maier SE, Takeda K. Usefulness of the apparent diffusion coefficient in line scan diffusion-weighted imaging for distinguishing between squamous cell carcinomas and malignant lymphomas of the head and neck. Am J Neuroradiol 2005;26:1186-92.

22. Dong C, Zheng Y, Li J, Wu ZJ, Yang ZT, Li XL, *et al*. A CT-based radiomics nomogram for differentiation of squamous cell carcinoma and non-Hodgkin's lymphoma of the palatine tonsil. Eur Radiol 2022;32:243-53.

23. Cheson BD, Fisher RI, Barrington SF, Cavalli F, Schwartz LH, Zucca E, *et al*. Recommendations for initial evaluation, staging, and response assessment of Hodgkin and non-Hodgkin lymphoma: the Lugano classification. J Clin Oncol 2014;32:3059.

24. Sehn LH, Salles G. Diffuse large B-cell lymphoma. N Engl J Med 2021;384:842-58.

25. Younes A, Hilden P, Coiffier B, Hagenbeek A, Salles G, Wilson W, *et al*. International Working Group consensus response evaluation criteria in lymphoma (RECIL 2017). Ann Oncol 2017;28:1436-47.

26. Tawfik MM, Monib AM, Yassin A, Ali SA. Comparison between RECIST and PERCIST criteria in therapeutic response assessment in cases of lymphoma. Egypt J Radiol Nucl Med 2020;51:82.